X89-36040

NASA Technical Memorandum 4116

Flutter of a Low-Aspect-Ratio Rectangular Wing

Stanley R. Cole

JUNE 1989

NASA

NASA Technical Memorandum 4116

Flutter of a Low-Aspect-Ratio Rectangular Wing

Stanley R. Cole
Langley Research Center
Hampton, Virginia

NASA
National Aeronautics and Space Administration
Office of Management
Scientific and Technical Information Division
1989

Summary

A flutter test of a low-aspect-ratio rectangular wing has been conducted in the Langley Transonic Dynamics Tunnel (TDT). The model used in this flutter test consisted of a rigid wing mounted to the wind-tunnel wall by a flexible, rectangular beam. The flexible support shaft was connected to the wing root and was cantilever mounted to the wind-tunnel wall. The wing had an aspect ratio of 1.5 based on wing semispan and an NACA 64A010 airfoil shape. The flutter boundary of the model was determined for a Mach number range of 0.5 to 0.97. The shape of the transonic flutter boundary was determined with actual flutter points obtained on both the subsonic and supersonic sides of the flutter bucket. The model exhibited a deep transonic flutter bucket over a narrow range of Mach number. At some Mach numbers, the flutter conditions were extrapolated using a subcritical response technique. In addition to the basic configuration, modifications were made to the model structure such that the first bending frequency was changed without significantly affecting the first torsion frequency. The experiment showed that increasing the bending stiffness of the model support shaft without affecting the torsional stiffness lowers the flutter dynamic pressure. Flutter analysis was conducted for the basic model as a comparison with the experimental results. This flutter analysis was conducted with planar, subsonic, lifting-surface (kernel function) aerodynamics using the k method for the flutter solution.

Introduction

The present study was conducted during the design phase for a flutter model to be tested in a cryogenic wind tunnel (ref. 1). A scaled version of the flutter model was tested in the Langley Transonic Dynamics Tunnel (TDT) to determine the flutter behavior that could be expected during the cryogenic flutter test. This present study was intended to verify the capabilities of the analytical tools used to design the cryogenic model and to characterize the behavior of the flutter model design in an effort to improve the safety of conducting the cryogenic flutter test. Subcritical response techniques were used at many Mach numbers to evaluate their validity for this type of model before applying the techniques in the cryogenic test.

The model design was based on a simple beam and rigid wing structure. The flexibility necessary to obtain flutter was provided through a support beam attached at the wing root. This type of mount raised questions about how the flutter model would behave should flutter be encountered and the amplitude grow until the support shaft was contacting the slot in the aerodynamic reflective plane at the wing root. This possibility was examined during this test by modifying the model support so that the bending stiffness changed with little effect on the torsional stiffness.

Symbols

A	response amplitude of subcritical response data peak, V
b	wing semispan, in.
b_o	half-chord length, in.
D	diameter, in.
E	Young's modulus of elasticity, lb/in^2
f	frequency, Hz
g	incremental damping
M	Mach number
M_o	model mass excluding support shaft, lb-sec^2/in.
q	dynamic pressure, lb/ft^2
R	radius, in.
V	velocity, in/sec
V_I	flutter-speed index, $V/(\omega_o b_o \sqrt{\mu})$
x	distance measured downstream from wing leading edge, in.
y	distance measured from wing root toward wingtip, in.
z	normalized modal deflections
μ	mass ratio, $M_o/(\pi b_o^2 b \rho)$
ρ	density, lb-sec^2/in^4
ω_o	reference frequency, rad/sec

Subscripts:

F	flutter result
i	vibration-mode order, 1,2,3,...

Test Apparatus

Wind Tunnel

The experimental flutter study was conducted in the Langley Transonic Dynamics Tunnel (TDT). The TDT is a transonic wind tunnel designed specifically for the testing of aeroelastic models (ref. 2). The facility is a continuous-circuit wind tunnel with a 16-ft-square test section. The tunnel is capable

of operating at pressures from near-vacuum to atmospheric pressure and from a Mach number of 0 to 1.2. The tunnel can operate in air or in a heavy gas (dichlorodifluoromethane). The present flutter test was conducted in the heavy-gas test medium. A unique safety feature of the TDT is a set of four quick-opening bypass valves that rapidly reduce the test-section Mach number and dynamic pressure when actuated. In the event of a model instability, such as flutter, these valves are used in an attempt to protect the wind-tunnel model.

Wind-Tunnel Model

The wind-tunnel model consisted of a "rigid" wing surface that was integrally connected to a flexible, rectangular support shaft at the root of the wing. The wing had zero sweep and an aspect ratio of 1.5 based on wing semispan. The wing has a semispan of 30 in. and a chord of 20 in. The airfoil was a symmetric NACA 64A010. The model is shown mounted in the TDT in figure 1. The construction of the wing is shown in figure 2. The wing stiffness was provided by a flat 0.25-in-thick aluminum plate (2024-T3) that was covered by balsa wood to provide the airfoil shape while minimizing the weight (fig. 3). The aluminum plate was rounded at the leading edge and tapered at the trailing edge to meet the airfoil shape. The aft 40 percent of the wing chord contained forty-nine 1.375-in. holes drilled through the aluminum plate to reduce the weight of the wing. These holes shifted the center of gravity of the wing to about 45 percent chord.

A rectangular flexure was attached to the wing root at the 30-percent-chord location to provide the model flexibility. This flexure was constructed of a 0.25-in. aluminum core cut from the same plate as the wing structure with two 0.0625-in. aluminum plates bonded and riveted to both sides. The thin plates added to the flexure were carried over a portion of the wing plate as an additional way to relieve stress concentrations at the wing root. The bond material resulted in a total shaft thickness of 0.393 in. with a shaft width of 2.25 in. The support flexure was 11.33 in. long from the wing root to the wind-tunnel wall support. The flexure was cantilevered to the wind-tunnel turntable to allow remote adjustment of the wing angle of attack during testing. A splitter plate (fig. 1) was mounted at the wing root to provide a symmetry reflection plane for the wing aerodynamics. Sufficient clearance was provided between the splitter plate, the wing root, and the support shaft to prevent contact during testing. The support shaft was instrumented with a bending-moment and torsion-moment strain gauge bridge near the cantilever point.

In addition to testing the basic wing for flutter, modifications were made to the model to investigate the effect of bending stiffness variation on flutter. These modifications consisted of cantilevering rectangular beam sections above the model support shaft and providing contact between the model and the beam at the centerline of the support shaft as shown in figure 4. The contact was electrically insulated and wired as an electrical switch to ensure that the beam remained in full contact with the model during low-amplitude flutter. Two modified configurations, a steel beam and an aluminum beam, were tested in this manner. These beams were 8.5 in. long from the cantilever to the point of contact on the model. Each beam had a cross section of 0.25 in. by 2.0 in. Since the contact with the beam was essentially through a single point near the elastic axis of the model, the bending stiffness of the basic model was increased while the torsional stiffness remained nearly constant.

Test Procedures

Ground Vibration Test

A ground vibration study was conducted on the wind-tunnel model to determine its natural frequencies and mode shapes. The model was excited in several of the primary modes by two methods: an impulse air shaker and an electromagnetic shaker. Results of the two methods correlated well. Mode shapes were also measured by two methods. The first method involved the use of sand to locate the node lines according to the scatter patterns developed while dwelling on a natural frequency. The second method utilized moving an accelerometer to locate the node lines of the natural vibration modes.

Wind-Tunnel Test

The flutter boundary for the model was approached by using two procedures during the wind-tunnel test. These two test procedures are shown in figure 5. The first procedure involved testing at a specific Mach number and at low dynamic pressure (relative to the predicted flutter dynamic pressure). Incremental increases in the dynamic pressure were then made at a constant Mach number to approach the flutter boundary (along path 1 in fig. 5). Subcritical response data were taken at constant tunnel flow conditions between each increase in dynamic pressure. These data were used to predict the flutter dynamic pressure by a subcritical response technique at each Mach number tested by this test procedure. This procedure is a relatively cautious manner of approaching the flutter conditions. It was used early in

the test to become familiar with the model behavior while approaching and entering the flutter condition.

The second procedure involved testing along a near-constant stagnation pressure line in the wind-tunnel operating boundary (along path 2 in fig. 5). This procedure was more time efficient and therefore was utilized for most of the testing once the typical behavior of the model was characterized. A combination of these two procedures was used for flutter testing on the supersonic side of the flutter bucket-shaped boundary (or flutter bucket). (See path 3 in fig. 5.) In order to test beyond the flutter bucket, a Mach number higher than the Mach number of the minimum point of the flutter bucket was first obtained by increasing flow speed as in the second procedure along a stagnation pressure line below the flutter-bucket minimum dynamic pressure. The dynamic pressure was then increased as in the first procedure at a constant Mach number. When the dynamic pressure became high enough to ensure that the test conditions were beyond the transonic flutter bucket, the Mach number was reduced along a constant stagnation pressure line (the reverse of the second procedure) until flutter was encountered.

The model was tested at a near-zero angle of attack throughout this experiment. Small changes in the angle of attack were made during the test so that the weight of the model was relieved (zero-g condition). This small positive angle of attack also ensured that the added beam stiffeners (for bending stiffness variation) remained in contact with the model while testing. An electrical connection wired through the model and contact point was used to further verify that the beam stiffeners remained in contact with the model until flutter occurred.

Subcritical Response Technique

The peak-hold subcritical response technique was used during this test (ref. 3) to predict the onset of flutter. The peak-hold technique utilizes frequency spectra data in which the highest amplitudes encountered in each sampled frequency band during the measurement period are stored throughout the frequency range of interest. The modes that are being excited during the wind-tunnel test produce much higher amplitudes than the response measured at off-mode frequencies. The peak-hold technique uses these peaks in the frequency spectra to "trace" the various modes as the dynamic pressure in the tunnel is increased. After the data are obtained at a given tunnel condition, the reciprocal of the peak amplitude for an excited mode is plotted against the dynamic pressure at which the measurement was made. This technique is continued as the dynamic pressure is incrementally increased toward the flutter condition. The amplitude of the mode tends to grow as the flutter dynamic pressure is approached so that the reciprocal of the amplitude approaches a value of zero at the flutter condition. Therefore, an extrapolation of the data will predict the flutter condition as the dynamic pressure at which the reciprocal of the response amplitude equals zero. Often, a straight-line extrapolation of the subcritical data gives a sufficient prediction of the flutter condition.

Analytical Tools

Several analytical computer programs were used to design the TDT flutter model. The results of these analyses also served as a guide in conducting the wind-tunnel test. Structural dynamic properties of the model were calculated using the engineering analysis language (EAL) finite-element-program package (ref. 4). Two-dimensional-plate elements were used to simulate the structural properties of the aluminum plate in the model. A drawing indicating the element arrangement developed in the finite element model is shown in figure 6. The elements of the support shaft and the area of increased thickness on the wing plate at the connection to the support shaft were modeled as aluminum with a thickness of 0.393 in. The remainder of the wing from the leading edge to the 60-percent-chord position was modeled as aluminum with a thickness of 0.25 in. The trailing-edge region of the finite element model was simulated by 0.25-in-thick plate elements with reduced values of Young's modulus of elasticity and density (compared with aluminum) to account for the holes drilled through the plate in this region. Also, the trailing-edge elements were shortened by 0.4 in. in the flow direction (in comparison with the physical model) to make an allowance for the trailing-edge taper in the aluminum plate. Nonstructural mass was added to the model to account for the weight of the balsa wood.

EAL was used to calculate natural frequencies, mode shapes, and generalized mass properties for the flutter model. Table 1 contains the calculated and measured natural frequencies for the first four vibration modes of the model, and table 2 shows the corresponding calculated mode shapes. The mode shapes are normalized by the EAL program so that all generalized masses have the numerical value of 1. Figure 7 shows the mode shapes graphically. Calculated mode shapes, generalized masses, and experimentally measured natural frequencies were then used in a flutter analysis software system, known as FAST (ref. 5), to calculate the flutter properties of the model. FAST calculates unsteady aerodynamic forces based on geometry and structural

dynamic properties using planar, subsonic, kernel-function, lifting-surface theory. Flutter instabilities are calculated using the k method (ref. 6).

Results and Discussion

Ground Vibration Test

Results of the ground vibration test are shown in figure 7 and table 1. Table 1 shows that the first two modal frequencies compare well with the calculated values. The third and fourth modal frequencies do not compare well, but these were not considered as important since analysis indicated that the flutter mechanism for this model was a classical coupling of the first bending and first torsion modes. Therefore, the flutter participation of the latter two modes would not be substantial. Figure 7 shows the comparison between calculated and measured node lines for the first four vibration modes. The agreement of analysis and experiment is good for the node lines of these modes. The agreement between both the node lines and the first two modal frequencies may indicate that the balsa wood was adding structural stiffness to the wing plate that was not accounted for in the analysis. This added stiffness would affect higher modes because of the increased involvement of wing plate flexibility.

Basic Wing Flutter

The experimental flutter boundary determined for the model in the TDT is shown in figure 8. Confirmed flutter points are indicated along with subcritical predictions of flutter. These flutter predictions, obtained by the peak-hold subcritical response technique, are shown in figure 9 for three Mach numbers. The plot for $M = 0.7$ includes the point at which flutter actually occurred (q_F) to verify the validity of the subcritical response technique for this model. Maximum dynamic pressure conditions obtained at Mach numbers where flutter was not reached are also shown to further verify the shape of the flutter boundary.

Analytical flutter results are presented for comparison with the experimental results. A summary of the flutter analysis results is given in table 3. Figure 10 shows a typical V-g plot as calculated by the flutter analysis routine. Figure 11 is a comparison of the experimental and the calculated flutter boundaries. The analysis is in good agreement with the experimental results and provides a conservative prediction of flutter between $M = 0.5$ and the transonic bucket. Figure 12 shows a comparison of the variation in modal frequencies as the flutter condition is approached both experimentally and as predicted by analysis. The experimental data shown in figure 12 represent the measured frequencies of the first two vibration modes at the corresponding dynamic pressure condition ($M = 0.7$). The analytical results were obtained through matched-point flutter analysis using the appropriate flow velocity and density for each dynamic pressure condition at which results were calculated.

Bending Stiffness Effects

The variation in the first two natural vibration frequencies due to the two structural modifications tested in the TDT are shown in table 4. The first bending frequency is shown to increase as either the aluminum beam or the steel beam is added to the structure of the model. On the other hand, the first torsion mode is not significantly affected. The wing-alone frequencies shown in table 4 are slightly different from the experimental results shown in table 1. Table 1 represents data obtained before the wind-tunnel test was made. Extensive flutter testing had been conducted before the bending stiffness effects were investigated, and numerous cracks had developed in the wing balsa wood. This may explain the slight variations in the natural frequencies. The flutter boundaries for the basic model and the two modifications are shown in figure 13. This shows that the shape of the flutter boundary is not significantly altered, although the steep trend through the transonic flutter bucket seems to be less drastic. Additional flutter data would be necessary to substantiate this trend, but the obvious effect of the additional bending stiffness is a lowered subsonic flutter boundary.

Conclusions

A flutter test of a simple low-aspect-ratio rectangular wing has been conducted in the Langley Transonic Dynamics Tunnel (TDT). The flutter boundary of the basic wing was determined for a Mach number range of 0.5 to 0.97. The shape of the transonic flutter bucket was well-defined. Some information on the recovery from the transonic flutter bucket was also obtained. In addition to the basic configuration, structural modifications were made to determine the effects of variation in the bending stiffness on the flutter characteristics of the model. The following conclusions can be drawn from this study:

1. The flutter boundary of the basic model exhibited a deep, well-defined flutter bucket over a narrow range of Mach number.

2. The analysis conducted for the basic model predicted the trend of the flutter boundary. The predicted flutter boundary was within 10 percent of the experimentally determined flutter dynamic pressures throughout the subsonic Mach number range.

3. The subsonic flutter boundary is lowered by increasing the first bending frequency without changing the first torsion frequency.

NASA Langley Research Center
Hampton, VA 23665-5225
May 9, 1989

References

1. Cole, Stanley R.: Exploratory Flutter Test in a Cryogenic Wind Tunnel. *J. Aircr.,* vol. 23, no. 12, Dec. 1986, pp. 904–911.
2. Reed, Wilmer H., III: *Aeroelasticity Matters: Some Reflections on Two Decades of Testing in the NASA Langley Transonic Dynamics Tunnel.* NASA TM-83210, 1981.
3. Sandford, Maynard C.; Abel, Irving; and Gray, David L.: *Development and Demonstration of a Flutter-Suppression System Using Active Controls.* NASA TR R-450, 1975.
4. Whetstone, W. D.: *EISI-EAL Engineering Analysis Language Reference Manual—EISI-EAL System Level 2091.* Engineering Information Systems, Inc., July 1983. *Volume 1: General Rules and Utility Processors.* *Volume 2: Structural Analysis—Primary Processors.*
5. Desmarais, Robert N.; and Bennett, Robert M.: *User's Guide for a Modular Flutter Analysis Software System (FAST Version 1.0).* NASA TM-78720, 1978.
6. Desmarais, Robert N.; and Bennett, Robert M.: An Automated Procedure for Computing Flutter Eigenvalues. *J. Aircr.,* vol. 11, no. 2, Feb. 1974, pp. 75–80.

Table 1. Calculated and Measured Natural Frequencies

Vibration mode		Natural frequency, Hz	
		Measured	Calculated
1	First bending	3.1	3.16
2	First torsion	14.1	14.4
3	Second bending	39.6	24.1
4	Second torsion	83.0	56.1

Table 2. Calculated Mode Shapes

Wing planform location		Normalized deflections			
x, in.	y, in.	z_1	z_2	z_3	z_4
0.0	0.0	0.96	−3.71	5.12	−7.54
↓	4.0	1.72	−4.35	6.60	−8.32
	8.0	2.54	−5.24	7.50	−8.02
	12.0	3.42	−6.30	7.31	−6.10
	16.0	4.35	−7.42	5.97	−2.56
	20.0	5.32	−8.53	3.66	2.14
	24.0	6.30	−9.60	6.68	7.22
	28.0	7.28	−10.60	−2.66	11.90
↓	30.0	7.78	−11.10	−4.37	14.00
4.9	0.0	1.07	−0.76	4.34	−2.30
4.0	4.0	1.80	−1.70	5.86	−4.21
↓	8.0	2.63	−2.32	6.47	−4.60
	12.0	3.52	−3.08	6.02	−3.93
	16.0	4.46	−3.93	4.51	−2.03
	20.0	5.42	−4.84	2.09	.90
	24.0	6.40	−5.76	−.95	4.41
	28.0	7.38	−6.68	−4.30	8.01
↓	30.0	7.87	−7.13	−6.02	9.80
7.1	0.0	1.10	0.51	4.17	−0.02
8.0	4.0	1.88	.93	5.36	−.01
↓	8.0	2.72	.67	5.71	−1.16
	12.0	3.61	.22	4.99	−1.86
	16.0	4.55	−.39	3.27	−1.73
	20.0	5.51	−1.11	.70	−.64
	24.0	6.49	−1.88	−2.44	1.22
	28.0	7.48	−2.70	−5.88	3.50
↓	30.0	7.97	−3.11	−7.64	4.72
12.0	0.0	1.15	3.77	4.35	6.32
↓	4.0	1.95	3.86	5.12	4.65
	8.0	2.80	3.84	5.14	2.46
	12.0	3.70	3.63	4.17	.20
	16.0	4.64	3.24	2.22	−1.57
	20.0	5.61	2.70	−.52	−2.44
	24.0	6.58	2.05	−3.81	−2.35
	28.0	7.57	1.33	−7.35	−1.54
↓	30.0	8.06	.96	−9.16	−.98
16.0	0.0	1.18	6.96	4.87	12.80
↓	4.0	2.01	7.13	5.12	9.81
	8.0	2.88	7.22	4.80	6.23
	12.0	3.78	7.17	3.56	2.23
	16.0	4.73	6.95	1.39	−1.53
	20.0	5.69	6.56	−1.57	−4.40
	24.0	6.67	6.02	−5.02	−6.07
	28.0	7.66	5.39	−8.68	−6.68
↓	30.0	8.15	5.06	−10.50	−6.79
19.6	0.0	1.22	10.00	5.24	18.30
↓	4.0	2.07	10.20	5.26	14.50
	8.0	2.94	10.40	4.71	9.63
	12.0	3.85	10.50	3.24	3.97
	16.0	4.80	10.40	.83	−1.64
	20.0	5.77	10.10	−2.35	−6.30
	24.0	6.75	9.62	−5.99	−9.45
	28.0	7.74	9.05	−9.77	−11.10
↓	30.0	8.23	8.74	−11.70	−11.50

Table 3. Calculated Flutter Results

M	q_F, lb/ft^2	f_F, Hz
0.40	140.6	8.19
.50	133.0	7.95
.60	127.3	7.59
.70	122.1	7.10
.80	114.3	6.51
.85	108.7	6.12
.90	100.6	5.65
.95	86.7	5.00

Table 4. Measured Natural Frequencies for Stiffness Variations

Configuration	f_1, Hz	f_2, Hz
Basic wing	3.0	13.8
Wing with aluminum beam	3.3	14.1
Wing with steel beam	3.5	13.8

L-82-10,016

Figure 1. Model mounted in the TDT.

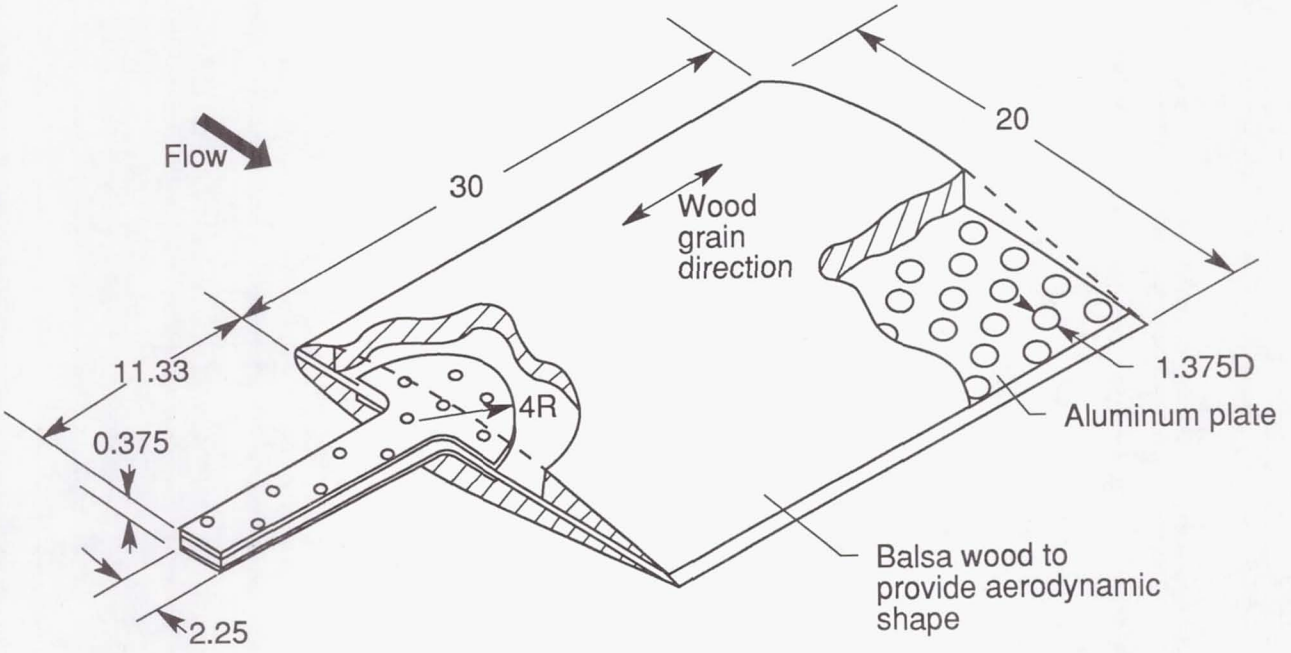

Figure 2. Cutaway drawing showing model construction. Dimensions are given in inches.

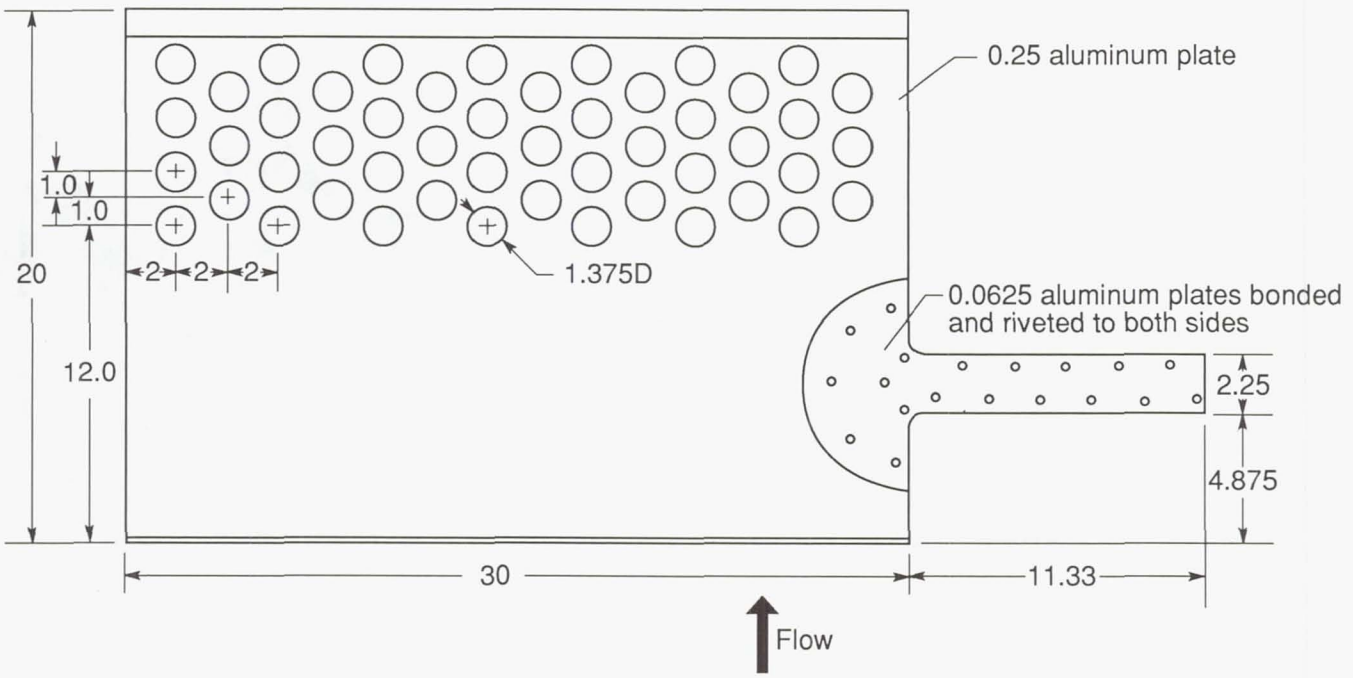

Figure 3. Aluminum plate construction. Dimensions are given in inches.

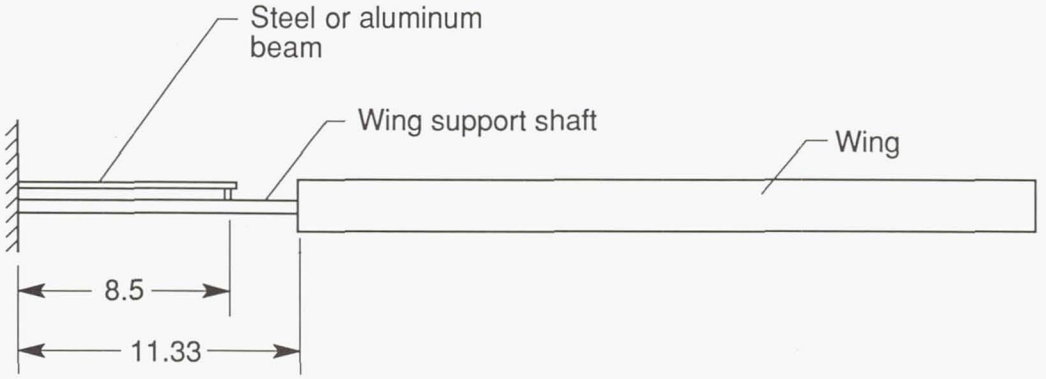

Figure 4. Contacting beam arrangement for bending stiffness variation. Dimensions are given in inches.

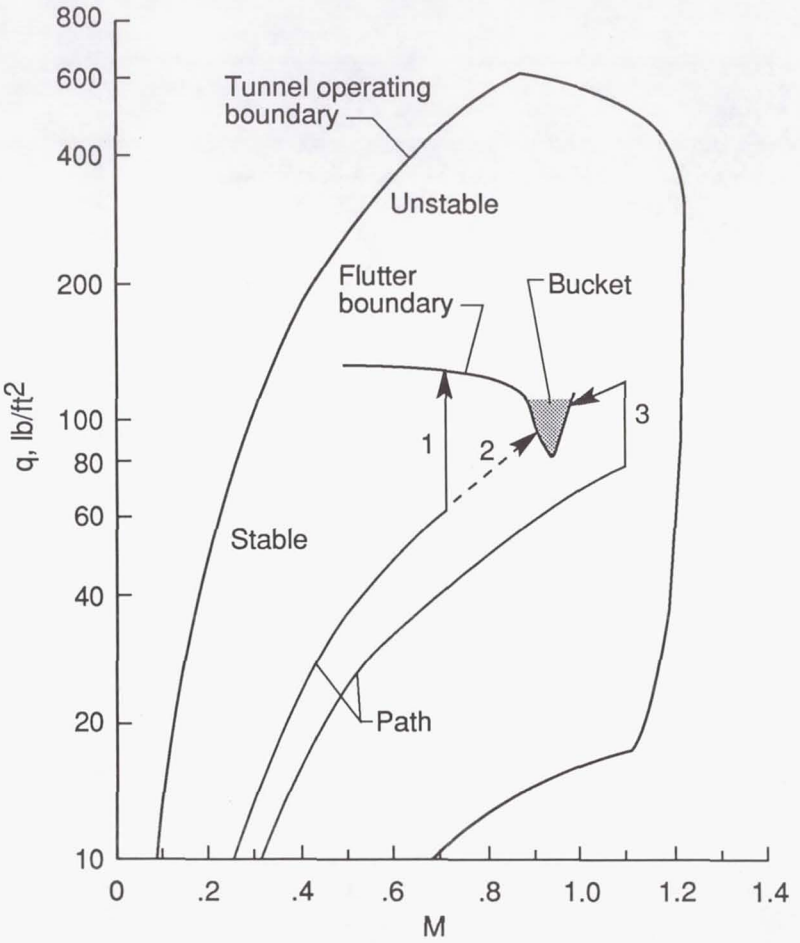

Figure 5. Flutter testing procedures used during the TDT test.

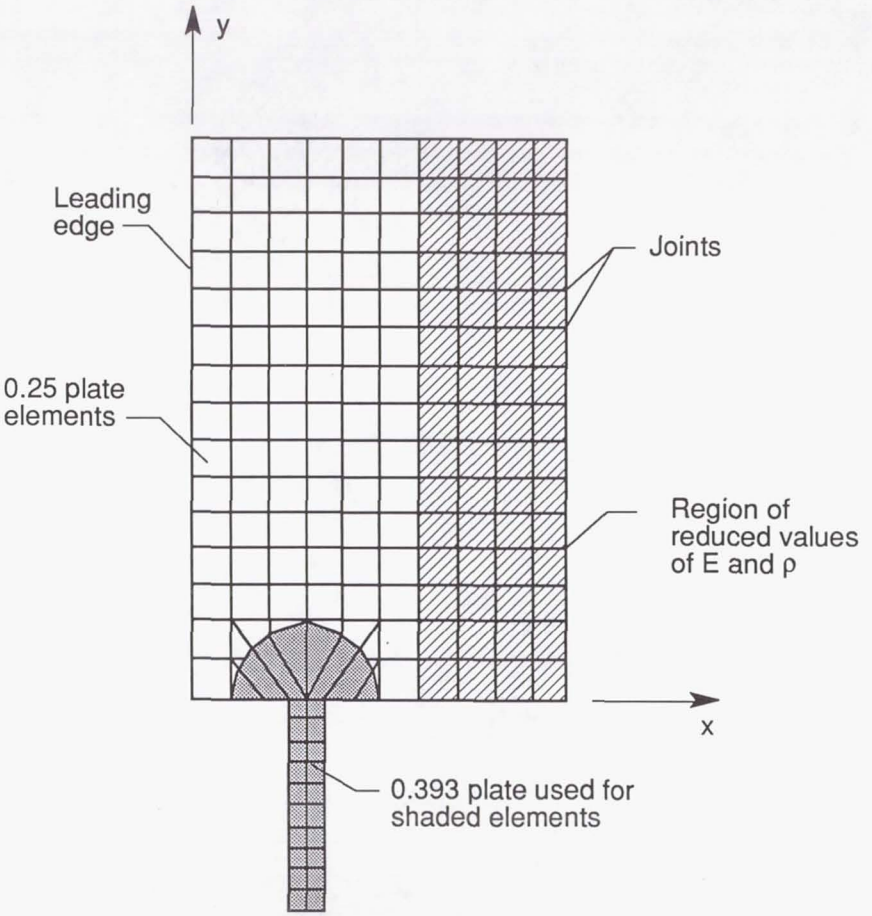

Figure 6. Finite element model. Dimensions are given in inches.

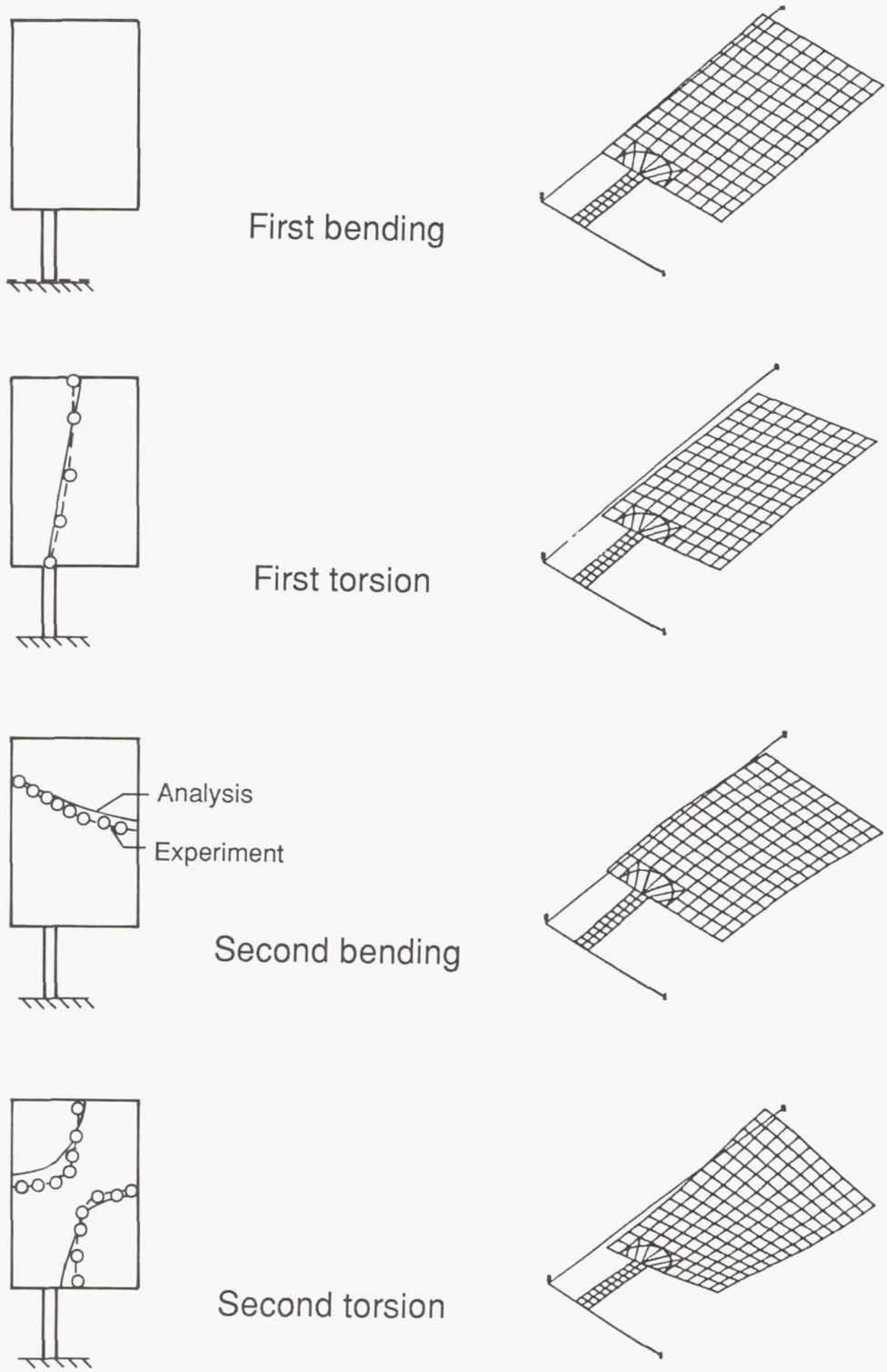

Figure 7. Calculated basic wing mode shapes and measured and calculated node lines.

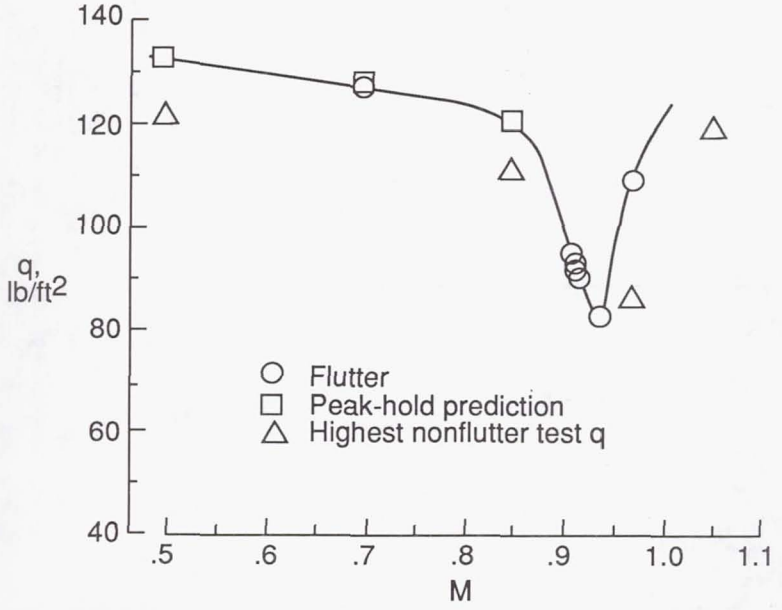

Figure 8. Experimental flutter results for basic wing.

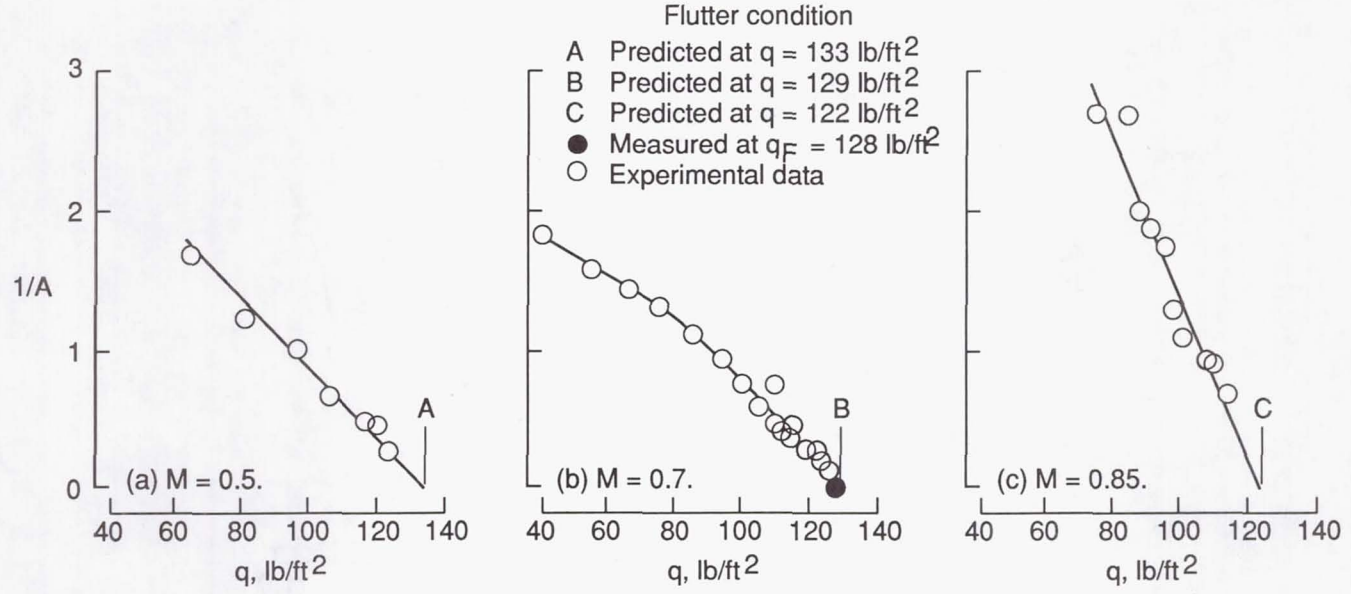

Figure 9. Subcritical response predictions of flutter.

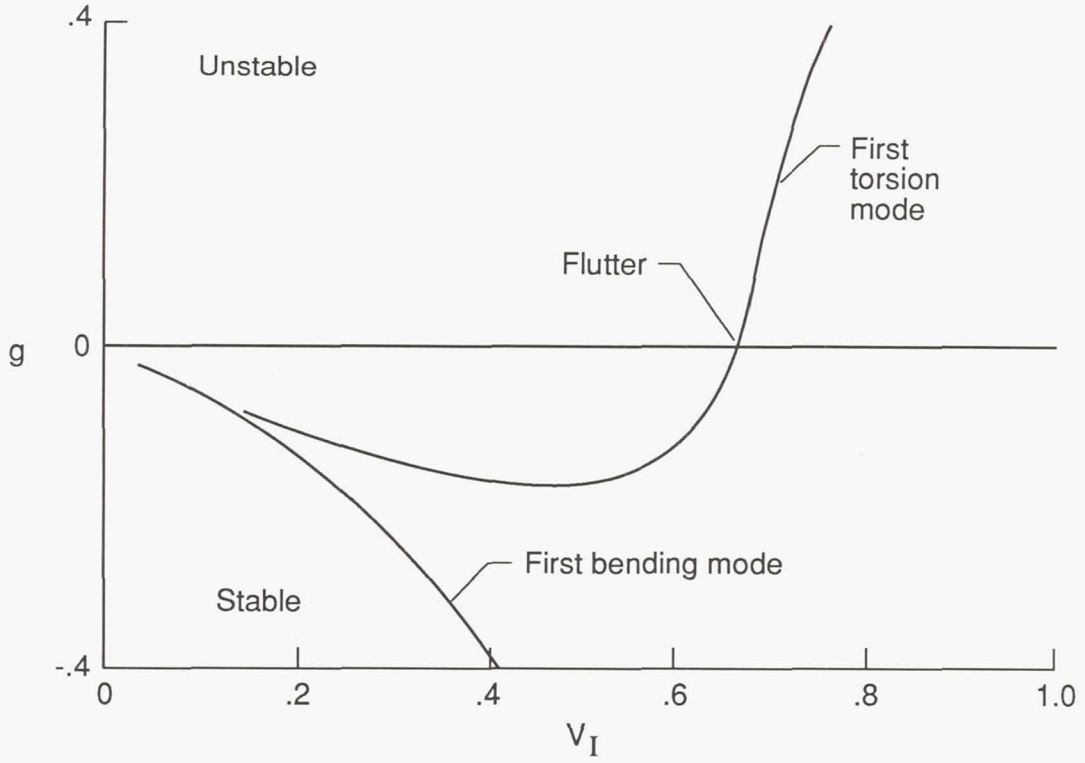

Figure 10. Typical calculated flutter results. $M = 0.7$; $\rho = 0.96 \times 10^{-7}$ lb-sec^2/in^4.

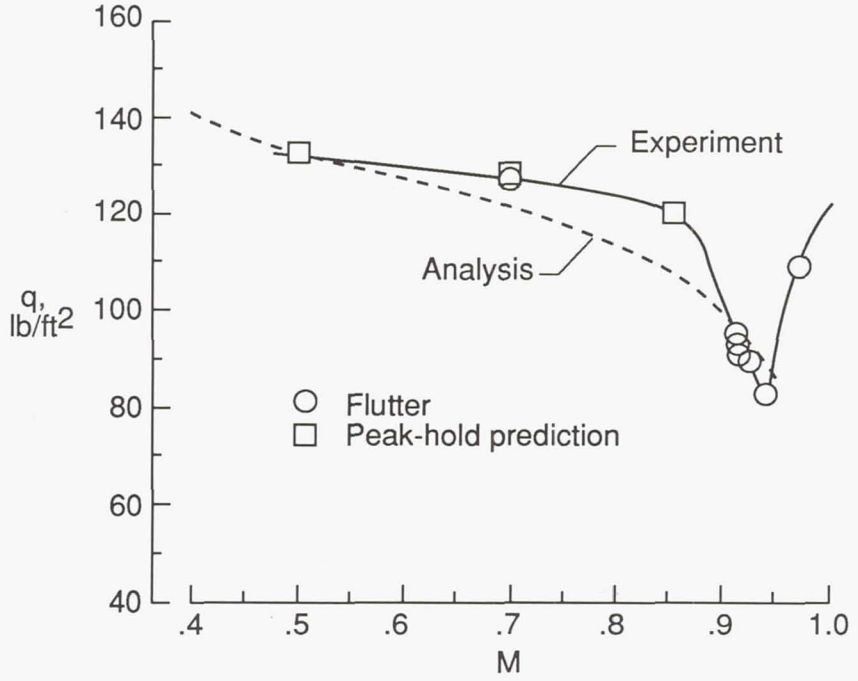

Figure 11. Experimental and calculated flutter boundaries for basic wing. Dashed line indicates curve fit of experimental data.

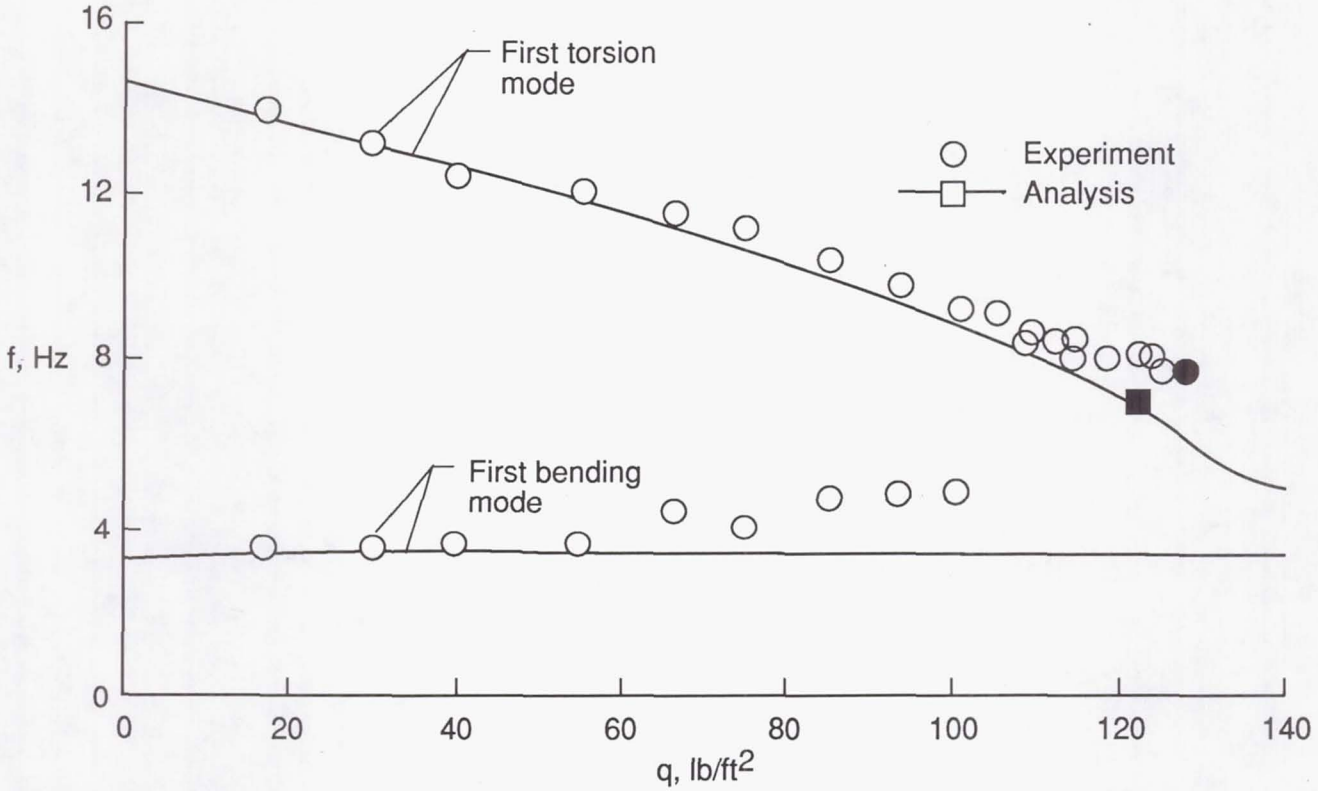

Figure 12. Subcritical frequency variation for basic wing at $M = 0.7$. Solid symbols indicate flutter condition.

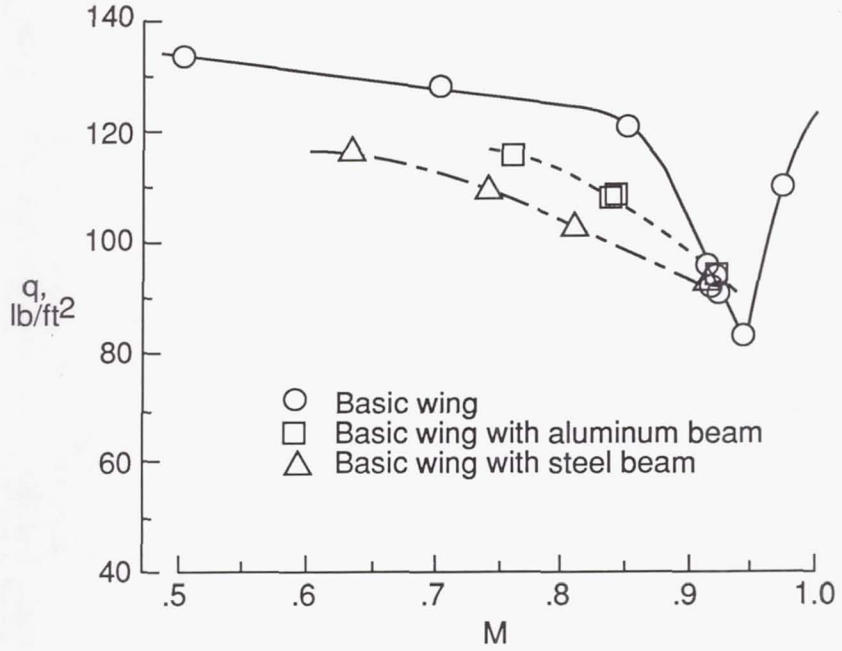

Figure 13. Effect of varying bending stiffness on flutter. Dashed lines indicate curve fits of experimental data.

NASA
National Aeronautics and Space Administration

Report Documentation Page

1. Report No.	2. Government Accession No.	3. Recipient's Catalog No.
NASA TM-4116		

4. Title and Subtitle	5. Report Date
Flutter of a Low-Aspect-Ratio Rectangular Wing	June 1989
	6. Performing Organization Code
7. Author(s)	8. Performing Organization Report No.
Stanley R. Cole	L-16544
	10. Work Unit No.
9. Performing Organization Name and Address	505-63-21-02
NASA Langley Research Center Hampton, VA 23665-5225	11. Contract or Grant No.
	13. Type of Report and Period Covered
12. Sponsoring Agency Name and Address	Technical Memorandum
National Aeronautics and Space Administration Washington, DC 20546-0001	14. Sponsoring Agency Code

15. Supplementary Notes

16. Abstract

A flutter test of a low-aspect-ratio rectangular wing was conducted in the Langley Transonic Dynamics Tunnel (TDT). The model used in this flutter test consisted of a rigid wing mounted to the wind-tunnel wall by a flexible, rectangular beam. The flexible support shaft was connected to the wing root and was cantilever mounted to the wind-tunnel wall. The wing had an aspect ratio of 1.5 based on the wing semispan and an NACA 64A010 airfoil shape. The flutter boundary of the model was determined for a Mach number range of 0.5 to 0.97. The shape of the transonic flutter boundary was determined. Actual flutter points were obtained on both the subsonic and supersonic sides of the flutter bucket. The model exhibited a deep transonic flutter bucket over a narrow range of Mach number. At some Mach numbers, the flutter conditions were extrapolated using a subcritical response technique. In addition to the basic configuration, modifications were made to the model structure such that the first bending frequency was changed without significantly affecting the first torsion frequency. The experiment showed that increasing the bending stiffness of the model support shaft through these modifications lowered the flutter dynamic pressure. Flutter analysis was conducted for the basic model as a comparison with the experimental results. This flutter analysis was conducted with subsonic lifting-surface (kernel function) aerodynamics using the k method for the flutter solution.

17. Key Words (Suggested by Authors(s))	18. Distribution Statement
Flutter Subcritical response technique Aeroelasticity Transonic	Unclassified–Unlimited Subject Category 05

19. Security Classif. (of this report)	20. Security Classif. (of this page)	21. No. of Pages	22. Price
Unclassified	Unclassified	16	A03

NASA FORM 1626 OCT 86

NASA-Langley, 1989

For sale by the National Technical Information Service, Springfield, Virginia 22161-2171